

# Spectral Imaging with a Programmable Light Source

Shoji Tominaga, Takahiko Horiuchi, Hirokazu Kakinuma and Akira Kimachi\*

Graduate School of Advanced Integration Science, Chiba University, Chiba, Japan

\* Department of Engineering Informatics, Osaka Electro-Communication University, Neyagawa, Japan

## Abstract

This paper proposes a high-speed spectral imaging system using an active spectral illumination for solving several problems in the current spectral imaging and finding effective applications. Our synchronous imaging system is constructed by combining a high-speed spectral light source and a high-speed monochrome camera. We describe the principle of illuminant control. Spectral-power distributions are generated as a time sequence. Then, we show some effective applications in the field of color imaging science and technology, which are (1) a quick estimation of surface-spectral reflectances, (2) a new method for colorimetry, and (3) a visual evaluation system under arbitrary illuminants, using the constructed imaging system. We demonstrate the usefulness of the proposed imaging system and the feasibility of the new technology for color imaging.

## Introduction

Spectral imaging technology is a useful technology that is now widespread in all fields related with visual information. Some situations requiring the spectral imaging technology are as follows:

- (1) A machine vision system based on trichromacy faces the limitation that a color camera with three bands RGB cannot always satisfy the color matching property of the human visual system.
- (2) The ability of color constancy demonstrates a subconscious ability to separate the illumination spectrum from the surface-spectral reflectance function. These spectral functions are not easily estimated from the RGB camera outputs.
- (3) Spectral analysis is often needed for the detailed analysis of natural scenes. Spectral synthesis is also required for the realistic image rendering under arbitrary viewing and illumination conditions.

A variety of multi-spectral imaging systems have been proposed for acquiring spectral information from a scene. Some typical systems are constructed by (1) using one or two additional color filters to a trichromatic digital camera [1],[2], (2) combining a monochrome camera and color filters with different spectral bands [3], (3) using narrow band interference filters, and (4) using a liquid-crystal tunable (LCT) filter to a monochromatic camera. It should be noted that most of these multi-spectral imaging systems have the mechanism of filtration on the camera side. Then the present imaging systems have several problems.

- (1) Image acquisition with changing filters consumes time.
- (2) It is not easy to design filters with appropriate spectral characteristics.
- (3) The accuracy of spectral estimation (and colorimetry) is inferior to use of a spectrophotometer (and spectroradiometer).

In this study, a high-speed spectral imaging system using an active spectral illumination is proposed for solving the above

problems and finding effective applications in the field of color imaging science and technology. We construct a synchronous imaging system by combining a high-speed spectral light source and a high-speed monochrome camera. The light source used in this study is a programmable spectral source which is capable of emitting arbitrary spectrum in high speed [4]. This system has the essential advantage of capturing spectral images without using filters in high frame rates. As a result, we can obtain spectral information of a scene quickly and precisely.

In this paper, we consider some applications using this imaging system. First, we devise a quick estimation of surface-spectral reflectances. The reflectance estimation is to solve an inverse problem for camera outputs. The difficulty in solving the problem on the traditional system is caused by eliminating the influence of illumination from the camera outputs. If the reciprocal function of the camera is projected onto surfaces as a time sequence of spectrum, we can obtain the surface-spectral reflectances with no computation for eliminating illumination. This direct spectral measurement has advantages in both computational time and estimation accuracy over previous indirect methods employing broad-band light sources such as light-emitting diodes (LEDs) [5], [6] or a xenon flash lamp [7].

Second, we propose a new method for colorimetry, instead of the traditional method based on colorimeter and spectrometer, where color values are obtained for a single location on an object surface. If the color-matching functions are projected onto object surfaces as spectral illuminants, the color values can be obtained at every point on the surface directly from the camera outputs. Brown et al. [8] produced the XYZ color-matching functions on a programmable light source of their own development, but did not give evaluation results. We evaluate the accuracy of color measurement with the color-matching functions realized on our system.

Third, we construct a visual evaluation system for objects in a scene under arbitrary illuminants. Human visual assessment of surface appearance is usually performed under limited light sources such as Illuminants A and D65. We can observe 3D object surfaces in a real scene by synthesizing illuminant with arbitrary spectral-power distribution. As a similar system, Mohan et al. [9] devised a projector that can change the spectral-power distribution of output light to a particular waveform, and used it to spectrally render a real scene. Their projector, however, lacks practical programmability because it requires mechanical replacement of individual transparent masks for each spectral waveform. In contrast, our system can realize spectral-power distribution of an arbitrary waveform in a very short time.

## Spectral Imaging System

Figure 1 shows an experimental setup for the proposed spectral imaging system. The system consists of a high speed

monochrome camera (Epix SV642M), a programmable light source (Optronic Laboratories OL490) [4], a Liquid light guide, and personal computers for controlling the camera and the light source.

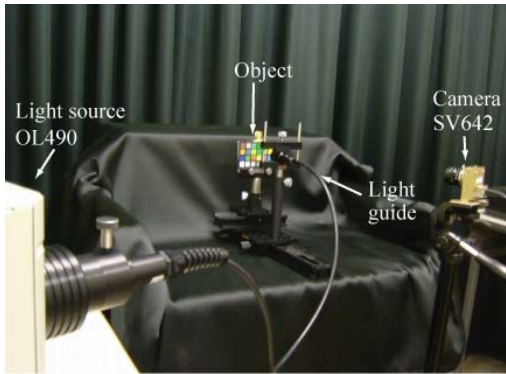


Figure 1 Experimental setup for the spectral imaging system.

### Light source

The principle of the programmable light source is depicted in Figure 2. It is composed of a xenon lamp source, a grating, a digital micromirror device (DMD) chip, and a liquid light guide. In this system, a light beam of xenon is separated by the grating into its constituent wavelengths. The wavelength and intensity information is controlled using the two-dimensional DMD chip, where one axis corresponds to the wavelength distribution of the spectrum, and the other axis to the intensity distribution [4], [8], [10]-[13]. The micromirrors on the DMD have two ON-OFF bistable states, which control the incident light. That is, the output intensity levels are controlled by the number of DLP mirrors toggled in the ON state. We use the chip of 1024x768 pixels, where the former number influences the wavelength resolution in the range of 380-780nm and the latter number determines the intensity quantization level. As an advantage of the DMD-based programmable light source, it can switch the output light spectrum much faster than a light source based on a liquid-crystal display [14].

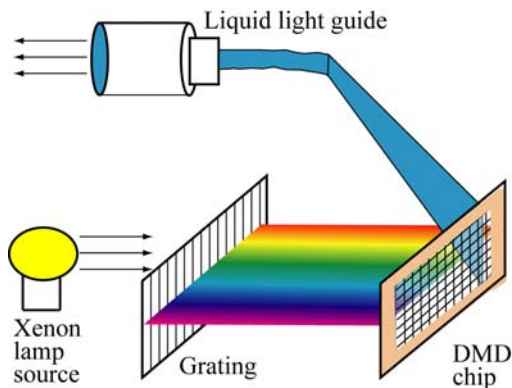


Figure 2 Principle of the programmable light source.

### Camera

The monochrome CMOS camera used in this paper provides 640x480 resolution and 8-bit quantization at about 200 frames per second (fps). We operate this camera with 320x240 resolution and 10-bit quantization at 20-200fps. Figure 3 shows the spectral-sensitivity function of the monochrome camera. Moreover we investigated a relationship between the input light intensities and the camera outputs. A good linear relationship is obtained at every wavelength.

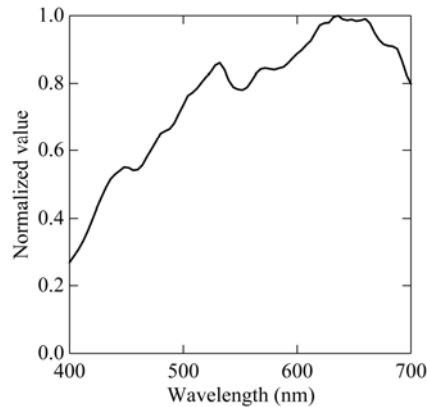


Figure 3 Spectral-sensitivity function of the monochrome camera.

### Synchronous imaging system

The camera and the light source are controlled by two computers in order to capture image sequences synchronously with the strobo light. Figure 4 shows the overview of the synchronous imaging system. Since the operation of the camera is much slower than the light source, the camera should be the master device in the relationship to the light source for their synchronization. Before capturing images, we have to create a sequence of frames forming lighting conditions such as wavelength, bandwidth, and relative intensity in advance [15]. The light source software then prepares a frame up for hardware triggering. When the camera starts observation of a scene, the RS644 strobe signal is output by the instruction from the control PC. The transfer module converts the signal into a TTL signal. The light source follows the TTL falling edge for illuminating next frame of the sequences.

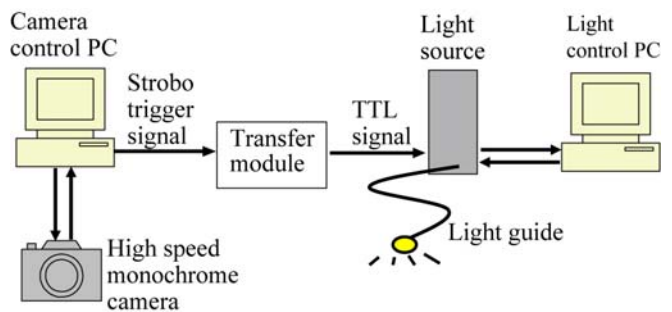
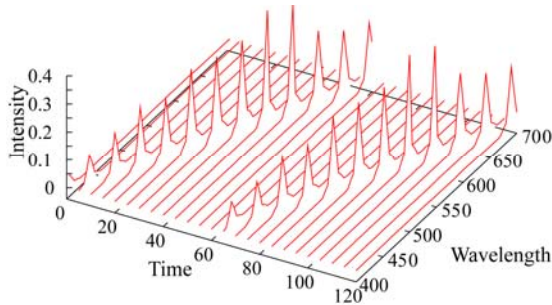


Figure 4 Overview of the synchronous imaging system.

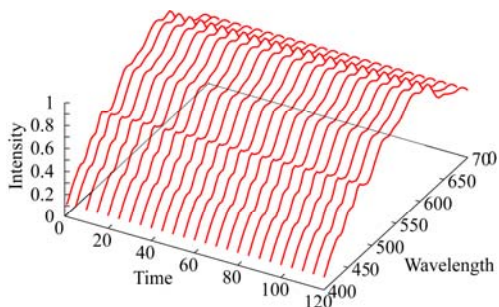
## Illuminant Control

### Time sequence of illuminant

The present light source system can produce emissions at a single wavelength or broad spectrum. We design the emission of a spectral function in two modes of time sequence: steady state and varying with time. In the steady-state mode, the same spectrum is generated at every time, while in the time-varying mode, different spectra can be generated at every time. Let  $E_{\lambda_i}(\lambda)$  be a spectral-power distribution emitted at a central wavelength  $\lambda_i$ . When we consider the time sequence  $(E_{\lambda_1}(\lambda), E_{\lambda_2}(\lambda), \dots, E_{\lambda_n}(\lambda))$ , the total emission over time produces the spectrum of  $E_{\lambda_1}(\lambda) + E_{\lambda_2}(\lambda) + \dots + E_{\lambda_n}(\lambda)$ . Figure 5 illustrates an example of spectral-power distributions generated as a time sequence. A set of single spectral functions with narrow width of wavelength is generated at an equal wavelength interval in the visible range. Figure 5 (a) is a 3D perspective view in the time varying mode, where different spectral functions are depicted in time series  $E_{\lambda_1}(\lambda, t_1), E_{\lambda_2}(\lambda, t_2), \dots, E_{\lambda_n}(\lambda, t_n)$ . Figure 5 (b) is the view in the steady-state mode, where the same spectrum is depicted at every time as  $E_{\lambda_1}(\lambda, t) + E_{\lambda_2}(\lambda, t) + \dots + E_{\lambda_n}(\lambda, t)$ .



(a) Time-varying mode



(b) Steady-state mode

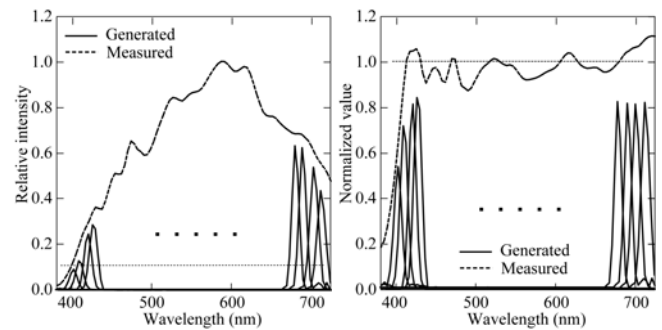
Figure 5 Spectral-power distributions generated as a time sequence.

### Production of spectral function

The programmable light source allows creation of our own spectra by changing the properties of wavelength, bandwidth, and relative intensity of multiple basis spectral functions from imported files. The basis spectra are usually selected from a set of spiky spectra with narrow bandwidth at different wavelengths. We note that the intensity of illuminant spectrum received at an object surface depends on the distance from the light source and the

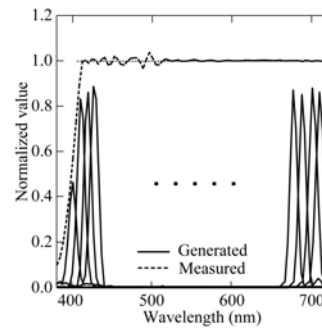
illumination angle. This change of intensity is nonlinear. Therefore, it is necessary to fix the imaging environment, including location and geometry of observation, to calibrate the output spectrum. First, we produced the calibrated illuminant of broad spectrum such as Illuminant A. The central wavelength, band width, and relative intensity for each basis spectrum were determined as an initial property. Then, the broad spectrum was generated in the steady state mode based on the imported property file. Since there is a discrepancy between the generated spectrum and the target spectrum, we have to adjust the intensity values in the property file for minimizing the discrepancy.

For instance, suppose that the target is a constant spectrum, which has also been a typical test target for other DMD-based programmable light sources [12], [13]. Figure 6 shows the process of spectral production. First we set the intensity value at every wavelength to the maximum value (100%) in the property file. The synthesized output spectrum is close to the spectral-power distribution of a xenon lamp as shown in Figure 6 (a), where the solid curves represent the spectra generated at the respective wavelength points, and the broken curve represents the illuminant spectrum directly measured by a spectro-radiometer. Next, the maximum intensity value is divided by the measurement at each wavelength for the purpose of producing the constant spectrum. However the resulting output spectrum is not always constant as shown in Figure 6 (b). In such a case, additional adjustments are needed [13]. We calculate an error between the target spectrum and the output spectrum at each wavelength. Then, we modify the intensity value iteratively for minimizing the error distance. Figure 6 (c) shows the output spectrum produced after ten iterations. We cannot produce a constant spectrum around 400nm because of the very dark region.



(a) First stage

(b) Second stage



(c) Final stage

Figure 6 Process for producing a constant spectrum.

## Applications

### Estimation of surface-spectral reflectance

The problem is to recover the surface-spectral reflectance of an object from the camera outputs by knowing the spectral sensitivity function of the camera. We solve the inverse problem effectively by using a time sequence of active illumination.

Let  $S(\lambda)$  and  $R(\lambda)$  be the surface-spectral reflectance function and the sensor-spectral sensitivity function, respectively. When an object surface is illuminated by a light source with spectrum  $E(\lambda, t)$ , the camera output at time  $t_i$  is described as

$$O(t_i) = \int S(\lambda)E(\lambda, t_i)R(\lambda)d\lambda. \quad (1)$$

If the light source is a narrow-band illuminant at the center wavelength  $\lambda_i$ , the camera output is rewritten as

$$O(t_i) = \int S(\lambda)E_{\lambda_i}(\lambda, t_i)R(\lambda)d\lambda = S(\lambda_i) \int E_{\lambda_i}(\lambda, t_i)R(\lambda)d\lambda. \quad (2)$$

Since the second term in the right-hand side of Eq.(2) is independent of an object surface, we can calculate it in advance as

$$c_i = \int E_{\lambda_i}(\lambda, t_i)R(\lambda)d\lambda. \quad (3)$$

When the surface is illuminated sequentially by the narrow-band spectrum with a moving center wavelength as shown in Figure 5 (a), the surface-spectral reflectance ( $S(\lambda_1), S(\lambda_2), \dots, S(\lambda_n)$ ) can be estimated from the time sequence of the camera outputs ( $O(t_1), O(t_2), \dots, O(t_n)$ ) as

$$S(\lambda_i) = O(t_i)/c_i \quad (i=1, 2, \dots, n). \quad (4)$$

It should be noted that we are not free to choose the intensity of the basis illuminant  $E_{\lambda_i}(\lambda, t_i)$ . If both illuminant intensity and spectral sensitivity are low, the captured image is very dark in the corresponding spectral band, so that the reflectance estimation becomes unreliable. Because of limitations of maximum illuminant intensity, the desired condition for stable spectral estimation is as follows:

$$c_i = \text{constant}, \quad E_{\lambda_i}(\lambda_i) \leq E_{\max}(\lambda_i), \quad (i=1, 2, \dots, n). \quad (5)$$

or for simplicity

$$E_{\lambda_i}(\lambda_i)R(\lambda_i) = \text{constant}, \quad E_{\lambda_i}(\lambda_i) \leq E_{\max}(\lambda_i), \quad (i=1, 2, \dots, n). \quad (6)$$

When the above condition is satisfied, we can obtain the estimate of the surface-spectral reflectance directly from the camera output sequence ( $O(t_1), O(t_2), \dots, O(t_n)$ ) without additional computation.

Figure 7 shows the illuminant spectrum which we designed for reflectance estimation in the present system, where the broken curve represents the target spectrum  $1/R(\lambda)$ , that is the reciprocal function of the camera spectral sensitivity. The bold curve represents the measurement of the illuminant spectrum produced by combining 61 basis illuminants emitted in time series at central wavelengths 400, 405, ..., 700 nm. The light source takes the maximum intensity in the dark region of 400-420 nm. In our

system, the constant  $c_i$  in Eq.(4) was derived as  $c_0=195, c_1=341, c_2=511, c_3=698, c_4=929, c_5=c_6=\dots=c_{61}=1023$ .

Figure 8 shows examples of experimental results using an X-Rite Mini ColorChecker. The estimated spectral curves of the spectral reflectances are depicted for two patches of red and blue. The broken curves  $S_m$  represent the direct measurements by a spectrophotometer, and the solid curves represent the estimation results of  $\hat{S} = (S(400), S(405), \dots, S(700))$ . Here,  $S_m$  and  $\hat{S}$  were normalized by the reference white. The numerical error was calculated between the spectral curves of the estimate  $\hat{S}$  and the measurement  $S_m$  as the RMSE

$$E = \left( \mathbf{E} \| S_m - \hat{S} \|^2 \right)^{1/2}. \quad (7)$$

The average RMSE for the 24 color patches in all was 0.024. This reliable reflectance estimation can be performed within a few second.

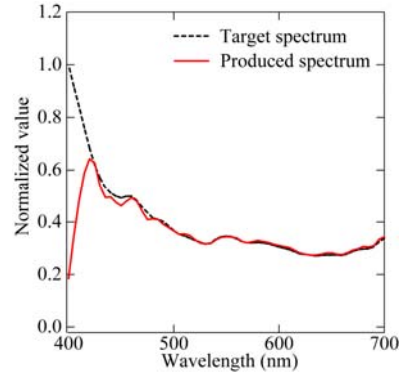


Figure 7 Illuminant spectrum designed for reflectance estimation

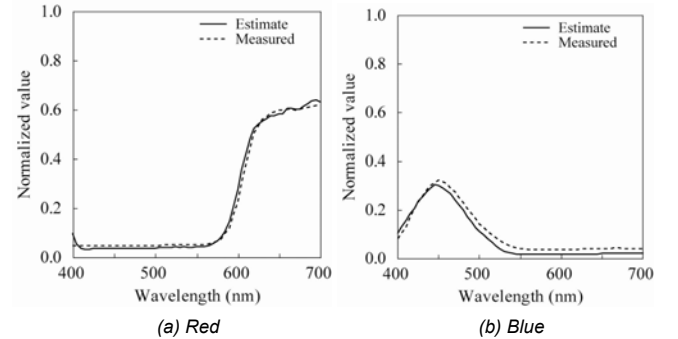


Figure 8 Examples of reflectance estimation results for two patches of a Color Checker.

### Colorimetry

The tristimulus values X, Y, and Z of an object surface are calculated as

$$\begin{bmatrix} X \\ Y \\ Z \end{bmatrix} = \int S(\lambda)E_T(\lambda) \begin{bmatrix} \bar{x}(\lambda) \\ \bar{y}(\lambda) \\ \bar{z}(\lambda) \end{bmatrix} d\lambda, \quad (8)$$

where  $E_T(\lambda)$  is a target illuminant, and  $(\bar{x}(\lambda), \bar{y}(\lambda), \bar{z}(\lambda))$  are the CIE color-matching functions. In the traditional technique of colorimetry, the above calculation is performed for light reflected from an object surface. Here we propose a new colorimetric

technique by projection of the color-matching functions as illuminant.

Let  $I(\lambda)$  be a linear combination of the basis spectra in the form

$$I(\lambda) = c_1 E_{\lambda_1}(\lambda) + c_2 E_{\lambda_2}(\lambda) + \dots + c_n E_{\lambda_n}(\lambda) . \quad (9)$$

Suppose that the set of whole basis spectra is projected to an object surface in the steady-state mode. The camera output is then described as

$$O = \int S(\lambda) I(\lambda) R(\lambda) d\lambda . \quad (10)$$

A comparison of Eq.(10) to Eq. (8) suggests that the tristimulus values can be obtained by the camera outputs if three conditions are satisfied as

$$I_x(\lambda)R(\lambda) = E_T(\lambda)\bar{x}(\lambda) , \quad I_y(\lambda)R(\lambda) = E_T(\lambda)\bar{y}(\lambda) ,$$

$$I_z(\lambda)R(\lambda) = E_T(\lambda)\bar{z}(\lambda) . \quad (11)$$

Therefore, the problem is reduced to determining the weights  $c_1, c_2, \dots, c_n$  for the basis spectra at  $\lambda_1, \lambda_2, \dots, \lambda_n$ , so that the illuminant spectra are coincident with the modified matching functions  $E_T(\lambda)\bar{x}(\lambda)/R(\lambda)$ ,  $E_T(\lambda)\bar{y}(\lambda)/R(\lambda)$ , and  $E_T(\lambda)\bar{z}(\lambda)/R(\lambda)$ . Since the present paper uses a monochrome camera, the camera outputs one of the tristimulus values at one time. Therefore, the tristimulus values can be obtained by the time sequence of the camera outputs  $(O(t_1), O(t_2), O(t_3))$ , where

$$\begin{aligned} O(t_1) &= \int S(\lambda) I_x(\lambda, t_1) R(\lambda) d\lambda , \\ O(t_2) &= \int S(\lambda) I_y(\lambda, t_2) R(\lambda) d\lambda , \\ O(t_3) &= \int S(\lambda) I_z(\lambda, t_3) R(\lambda) d\lambda . \end{aligned} \quad (12)$$

Note that the tristimulus values are obtained at every pixel point in a scene.

Figure 9 shows the illuminant spectra  $I_x(\lambda, t_1)$ ,  $I_y(\lambda, t_2)$ , and  $I_z(\lambda, t_3)$  produced for obtaining the tristimulus values under a constant illuminant, by the present system. The broken curves represent the modified color-matching functions  $\bar{x}(\lambda)/R(\lambda)$ ,  $\bar{y}(\lambda)/R(\lambda)$ , and  $\bar{z}(\lambda)/R(\lambda)$  of the target spectra. The bold curves represent the measurements of the produced spectra. We performed an experiment of colorimetry. The above illuminants were projected to the color checker. The 24 color patches in all were measured by repeating the projection to the patch of 2x2 at the same time. The accuracy was evaluated by color difference. The average of CIE-L\*a\*b\* difference were 2.68 for the 24 patches. The color difference of four color patches in Sec.4.1 were 2.97 for red, 1.23 for green, 1.18 for blue, and 3.78 for yellow. The projection time for each 2x2-patches was less than 10 milliseconds.

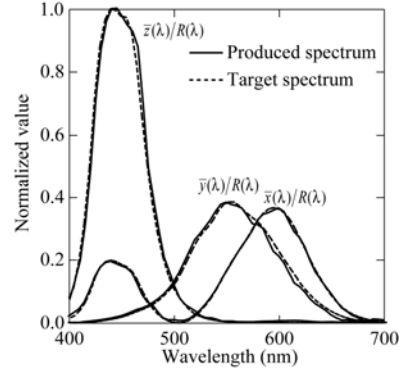


Figure 9 Illuminant spectra produced for ob the tristimulus values under a constant illuminant.

### Visual evaluation

In the conventional visual evaluation experiments, we often used standard light sources such as Illuminants A and D65, or used a combination of some light sources. Therefore, the feasibility of illuminant-spectral shape is extremely limited. The proposed imaging system provides us an experimental environment to observe object surfaces in a real scene under illuminant with arbitrary spectral-power distribution. Besides, the color appearance can be compared with the color values obtained from the camera by the procedure in the previous subsection. So this system is available for various fields with visual evaluation on object appearance.

Figure 10 shows the produced illuminant spectral distributions for Illuminants A and D65. The produced spectra are almost coincident with the target spectra. This suggests a good performance of our system and algorithms. Figure 11 demonstrates appearances of the ColorChecker Chart under the two illuminants in the real experimental environment.

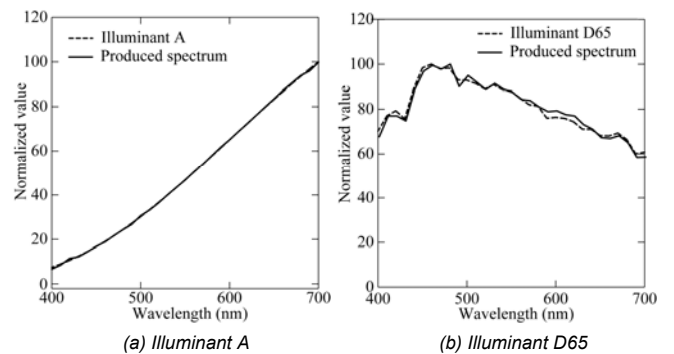
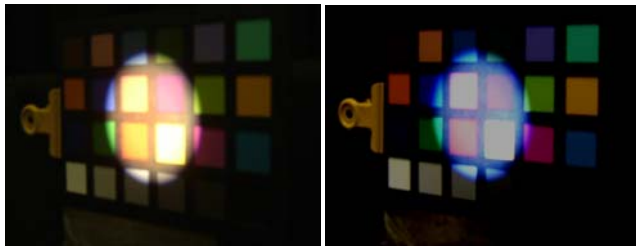


Figure 10 Illuminant spectral distributions produced for Illuminants A and D65.



(a) Illuminant A

(b) Illuminant D65

Figure 11 Appearances of the ColorChecker Chart under illuminants A and D65

## Conclusions

This paper has proposed a high-speed spectral imaging system using an active spectral illumination. Our synchronous imaging system was constructed by combining a high-speed spectral light source and a high-speed monochrome camera. We described the principle of illuminant control. Spectral-power distributions were generated as a time sequence. Then we showed some effective applications in the field of color imaging science and technology, which were (1) a quick estimation of surface-spectral reflectances, (2) a new method for colorimetry, and (3) a visual evaluation system under arbitrary illuminants, using the constructed imaging system.

We have demonstrated the usefulness of the proposed imaging system and the feasibility of the new technology for color imaging. The proposed technology may be epoch-making in the field of spectral color imaging, and have a potential ability. Hence many practical applications are expected as a future work.

## References

- [1] F.H. Imai and R.S. Berns, "Spectral estimation using trichromatic digital camera," Proc. of International Symp. Multispectral Imaging and Color Reproduction for Digital Archives, pg.42, (1999).
- [2] S. Tominaga, T. Fukuda, and A. Kimachi, "A high-resolution imaging system for omnidirectional illuminant estimation," Jour. Imaging Sci. and Technol., 52(4), 040907-1 (2008).
- [3] S. Tominaga and T. Fukuda, "Omnidirectional scene illuminant estimation using a multispectral imaging system," Proc. SPIE, 5667, pg. 128, (2007).

- [4] A. Fong, B. Bronson and E. Wachman, "Advanced photonic tools for hyperspectral imaging in the life sciences," SPIE Newsroom, (2008).
- [5] J.-I. Park, M.-H. Lee, M. D. Grossberg and S. K. Nayar, "Multispectral imaging using multiplexed illumination," Proc. ICCV, pg. 14, (2007).
- [6] F. Xiao, J. M. DiCarlo, P. B. Catryse and B. A. Wandell, "Image analysis using modulated light sources," Proc. SPIE, 4306, pg. 22, (2001).
- [7] J. M. DiCarlo, F. Xiao and B. A. Wandell, "Illuminating Illumination," Proc. CIC, pg. 27, (2001).
- [8] S. W. Brown, J. P. Rice, J. E. Neira, B. C. Johnson and J. D. Jackson, "Spectrally tunable sources for advanced radiometric applications," J. Res. of the National Institute of Standards and Technology, 111(5), 401 (2006).
- [9] A. Mohan, R. Raskar and J. Tumblin, "Agile spectrum imaging: programmable wavelength modulation for cameras and projectors," Computer Graphics Forum, 27(2), 709 (2008).
- [10] J. P. Rice, S. W. Brown, B. C. Johnson and J. E. Neira, "Hyperspectral image projectors for radiometric applications," Metrologia, 43, S61 (2006).
- [11] J. P. Rice, S. W. Brown, J. E. Neira and R. R. Bousquet, "A hyperspectral image projector for hyperspectral imagers," Proc. SPIE, 6565, pg. 65650C-1, (2007).
- [12] N. MacKinnon, U. Stange, P. Lane, C. MacAulay and M. Quatrevalet, "Spectrally programmable light engine for in vitro or in vivo molecular imaging and spectroscopy," Appl. Opt., 44(11), 2033 (2005).
- [13] C. H. Chuang and Y. L. Lo, "Digital programmable light spectrum synthesis system using a digital micromirror device," Appl. Opt. 45(32), 8308 (2006).
- [14] M. Hauta-Kasari, K. Miyazawa, S. Toyooka and J. Parkkinen, "Spectral vision system for measuring color images," J. Opt. Soc. Am. A, 16(10), 2352 (1999).
- [15] OL490 Agile Light Source Manual, Optronics Laboratories, (2008).

## Author Biography

*Shoji Tominaga received the B.E., M.S., and Ph.D. degrees in electrical engineering from Osaka University, Japan, in 1970, 1972, and 1975, respectively. From 1976 to 2006, he had been with Osaka Electro-Communication University. Since 2006, he is a professor at Graduate School of Advanced Integration Science, Chiba University. During the 1987-1988 academic years he was a Visiting Scholar at the Department of Psychology, Stanford University. He is a fellow of IEEE, IS&T and SPIE.*